Design of Input Shapers using Modal Cost for Multi-mode Systems

Ravi Kumar[a], Tarunraj Singh[,b]

[a]Department of Mechanical & Aerospace Engineering, University at Buffalo, Buffalo, NY 14260
[b]Department of Mechanical & Aerospace Engineering, University at Buffalo, Buffalo, NY 14260

Abstract

This paper presents two techniques for the determination of modal weights for the design of robust input shapers for multi-mode systems. The weights for the first technique are derived based on the scaling factor for the potential energy in each mode, such that the modal displacement is the same. The second technique exploits the *modal cost* analysis which uses the angle between the right eigenvectors and the row vectors of the output matrix to determine the contribution of each mode to the output. Two examples are used to illustrate the improvement in performance of the modal weighted minimax shapers compared to the traditional minimax shaper which equally weighs all the modes.

Key words: Input Shaping, Minimax design, Multi-mode, Vibration Control

1. Introduction

Parasitic vibrations can decrease the performance of maneuvering structures such as cherry pickers, flexible arm robot (Remote Manipulator System of the Space Shuttle), cranes [1, 2], etc., where the goal is to move from one position of rest to another position of rest. There is a large body of work which deals with shaping the reference input to these dynamical system so as to minimize residual vibrations. The posicast controller [3], Input Shaper [4], Time-Delay filter [5], use a superposition idea to cancel oscillations. Input Shaping refers to the process of convolving a series of impulses with a reference profile to generate a shaped input. Time-Delay filtering refers to the process of modifying the reference input by combining a weighted set of delayed reference input. The Input shaper and time-delay filter are essentially identical and will be used interchangeably in this paper. The design of Input Shaper and Time-Delay filters have been extended to exploit knowledge of the domain of uncertainty to arrive at shaped profiles which generate reasonable performance over the entire domain of uncertainty. Here, the terminal constraint are not equality constraints, rather they are inequality constraints that requires the terminal states to lie within a set which include the desired final position. For a multi-mode system, the traditional approach has been to cascade input-shapers/time-delay filter designed for each mode to satisfy terminal constraints. For problems which include worst case design (minimax time-delay filter [6]), residual energy which incorporates all the modes has been used to design the filter to shape the reference input. The Specified Insensitivity (SI) [8] Input Shaper for the multi-mode case can be designed by

including SI constraints for each of the modes. This can be represented as:

$$V(\omega_i, \zeta_i) = e^{-\zeta_i \omega_i} \sqrt{\mathcal{C}^2 + \mathcal{S}^2} < V_{tol} \ \forall i = 1, 2, \dots \tag{1}$$

$$\mathcal{C} = \sum_{j=1}^{n} A_j e^{-\zeta_i \omega_i} cos(\omega_i \sqrt{1 - \zeta_i^2} t_j) \tag{2}$$

$$\mathcal{S} = \sum_{j=1}^{n} A_j e^{-\zeta_i \omega_i} sin(\omega_i \sqrt{1 - \zeta_i^2} t_j) \tag{3}$$

where A_j and t_j are the magnitude and time of application of the impulses of the input shaper. However, if the goal is to target a specific output which has non-equal contribution of various modes, the Varying-Amplitude-Contribution SI [9] differentially weights each of the $V(\omega_i, \zeta_i)$ in the design process. For a two mode example, the constraints are represented as:

$$\alpha V_{tol}^1 + (1 - \alpha) V_{tol}^2 \ < \ V_{tol}, \quad \alpha \in \begin{bmatrix} 0 & 1 \end{bmatrix} \tag{4}$$

$$V(\omega_1, \zeta_1) \ < \ V_{tol}^1, \omega_1 \in \begin{bmatrix} \omega_1^{lb} & \omega_1^{ub} \end{bmatrix} \tag{5}$$

$$V(\omega_2, \zeta_2) \ < \ V_{tol}^2, \omega_2 \in \begin{bmatrix} \omega_2^{lb} & \omega_2^{ub} \end{bmatrix} \tag{6}$$

where α is selected based on the contribution of each mode and ω_i^{lb} and ω_i^{ub} correspond to the lower and upper bounds of ω_i respectively. V_{tol} represents the threshold for the permitted residual energy. V_{tol}^1 is arbitrarily selected to be some fraction of V_{tol} and V_{tol}^2 is consequently calculated as:

$$V_{tol}^2 = \frac{V_{tol} - \alpha V_{tol}^1}{1 - \alpha} \tag{7}$$

Experimental results were used to determine V_{tol}^1 and V_{tol}^2 and the resulting input shaper was shown to have better performance compared to the traditional two-mode SI shaper [8]. One can conjecture that as the number of modes increases, the selection of the weights α_i and the permitted V_{tol}^i can become cumbersome.

This paper endeavors to develop an analytical approach for the determination of weighting factors for vibratory modes which can subsequently be used to design robust input shapers which minimize the worst case performance over the entire domain of uncertainty. Consider the three mass-spring system shown in Figure 1 by the solid lines. The second order model of the system is:

$$\begin{bmatrix} 1 & 0 & 0 \\ 0 & 1 & 0 \\ 0 & 0 & 1 \end{bmatrix} \begin{Bmatrix} \ddot{x}_1 \\ \ddot{x}_2 \\ \ddot{x}_3 \end{Bmatrix} + \begin{bmatrix} 1 & -1 & 0 \\ -1 & 2 & -1 \\ 0 & -1 & 1 \end{bmatrix} \begin{Bmatrix} x_1 \\ x_2 \\ x_3 \end{Bmatrix} = \begin{bmatrix} 1 \\ 0 \\ 0 \end{bmatrix} u. \tag{8}$$

The three modes of this system

$$\begin{Bmatrix} x_1 \\ x_2 \\ x_3 \end{Bmatrix} = \begin{Bmatrix} 0.5774 \\ 0.5774 \\ 0.5774 \end{Bmatrix}, \begin{Bmatrix} -0.7071 \\ 0 \\ 0.7071 \end{Bmatrix}, \begin{Bmatrix} 0.4082 \\ -0.8165 \\ 0.4082 \end{Bmatrix} \tag{9}$$

are shown in the same figure by dashed lines. The frequencies corresponding to the three modes are: $\omega_i = \begin{bmatrix} 0 & 1 & \sqrt{3} \end{bmatrix}$. If the output of interest is the displacement of the third mass, the output equation is:

$$z = \begin{bmatrix} 0 & 0 & 1 \end{bmatrix} \begin{Bmatrix} x_1 \\ x_2 \\ x_3 \end{Bmatrix} \tag{10}$$
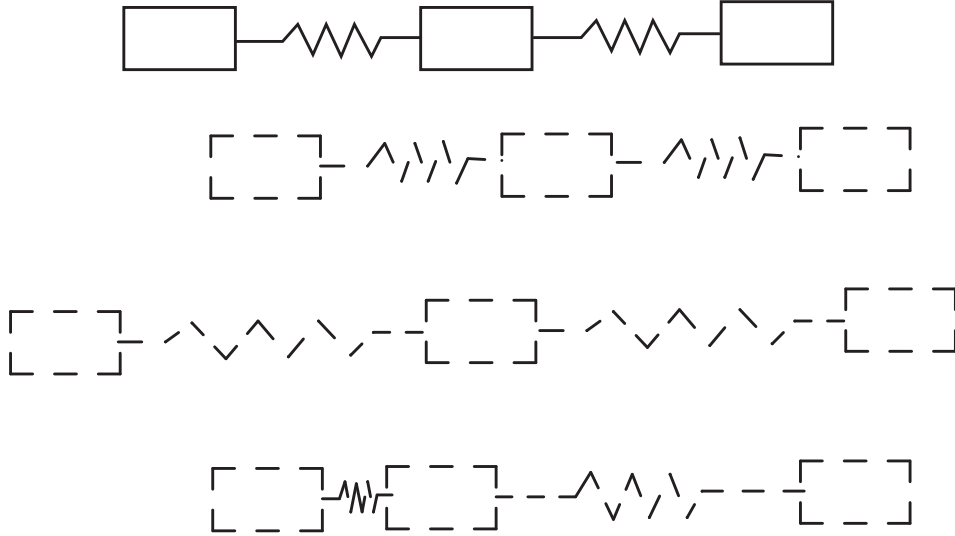
2

Figure 1: 3 Mass-Spring Systems and Mode Shapes

The system model and output equation can be rewritten in modal form as:

$$\begin{bmatrix} 1 & 0 & 0 \\ 0 & 1 & 0 \\ 0 & 0 & 1 \end{bmatrix} \begin{Bmatrix} \ddot{y}_1 \\ \ddot{y}_2 \\ \ddot{y}_3 \end{Bmatrix} + \begin{bmatrix} 0 & 0 & 0 \\ 0 & 1 & 0 \\ 0 & 0 & 3 \end{bmatrix} \begin{Bmatrix} y_1 \\ y_2 \\ y_3 \end{Bmatrix} = \begin{bmatrix} 1 \\ 0 \\ 0 \end{bmatrix} u. \tag{11}$$

and

$$z = \begin{bmatrix} -0.5774 & 0.7071 & 0.4082 \end{bmatrix} \begin{Bmatrix} y_1 \\ y_2 \\ y_3 \end{Bmatrix} \tag{12}$$

which clearly indicates that the second mode's contribution is the largest and the third mode's is the smallest. These modal contributions can be used to relatively weight the modal energies to formulate a cost function whose maximum can be minimized over the uncertain domain.

2. Minimax time-delay control

This section reviews the minimax time delay input shaper design proposed by Singh [6]. Here the goal is to design a shaped reference profile such that the vibrations at the end of a pre-specified maneuver are minimized. Consider the second order linear mechanical system of the form

$$M\ddot{\mathbf{x}} + C(\mathbf{p})\dot{\mathbf{x}} + K(\mathbf{p})\mathbf{x} = D\mathbf{u} \tag{13}$$

$$\mathbf{y}_o = C_o \mathbf{x} \tag{14}$$

where the $n \times n$ mass matrix M is positive definite, the $n \times n$ damping and stiffness matrices C and K are positive semi-definite. D is the $n \times m$ control influence matrix, $\mathbf{x} \in \mathbb{R}^n$ is the configuration vector, $\mathbf{u} \in \mathbb{R}^m$

3

is control vector, C_o is the output matrix and $\mathbf{y}_o$ is the output. $\mathbf{p}$ is a vector of uncertain parameters whose range of uncertainty is:

$$p_i^{lb} < p_i < p_i^{ub}. \tag{15}$$

For rest to rest maneuvers from some prescribed initial state to final state, the time delay filter is parameterized with the following transfer function:

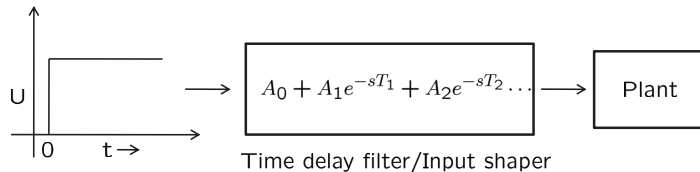$$G(s) = A_0 + A_1 e^{-sT_1} + A_2 e^{-sT_2} + \cdots \tag{16}$$

Figure 2: Block diagram of Time delay / Input shaping based control

Figure 2 shows the block diagram implementing the point-to-point maneuver. For designing a robust filter i.e., finding the parameters $A_i s$ and $T_i s$ in equation 16, the minimax optimization procedure proposed in [6] uses residual energy of the system at the end of maneuver defined as

$$V_{res} = \frac{1}{2}\dot{\mathbf{x}}^T M \dot{\mathbf{x}} + \frac{1}{2}(\mathbf{x} - \mathbf{x}_r)^T K (\mathbf{x} - \mathbf{x}_r) \tag{17}$$

as the cost function where x_r corresponds to the desired reference position. The following minimax optimization problem is solved to find the unknown parameters

$$\min_{A_i, T_i} \max_{p_i} V_{res} \tag{18}$$

where the knowledge of the distribution of the parameter uncertainties can be incorporated into equation 18 by weighting the cost V_{res} with the probability distribution function of the uncertain variables [12]. It should be noted that the minimax optimization problem results in different solutions for different maneuvers. A lookup table of the solutions of the minimax problem as a function of the maneuver can be used for real-time implementation.

3. Robust filter design using weighting factors based on modal displacement

In the approach presented in section 2, the contribution to the residual energy of all the modes of the system are weighted equally. To better control the plant output, we can scale the contributions of each mode to the residual energy based on their contribution to the output. To determine these scaling factors, we transform the system described by equation 13 to the modal form by introducing a coordinate transformation of the form

$$\mathbf{x}(t) = \Phi \mathbf{y}(t) \tag{19}$$

where Φ is $n \times n$ similarity transformation matrix obtained by solving the eigen value problem associated with the mass and the stiffness matrices. The residual energy of the transformed system can then be expressed as

$$V = \frac{1}{2}\dot{\mathbf{y}}^T \tilde{M}\dot{\mathbf{y}} + \frac{1}{2}(\mathbf{y} - \mathbf{y}_r)^T \tilde{K}(\mathbf{y} - \mathbf{y}_r) \tag{20}$$

where $\tilde{M}$ and $\tilde{K}$ are the transformed mass and stiffness matrices given by

$$\tilde{M} = \Phi^T M \Phi = I \tag{21}$$

$$\tilde{K} = \Phi^T K \Phi = \begin{Bmatrix} \omega_1^2 & 0 & 0 & \dots & 0 \\ 0 & \omega_2^2 & 0 & \dots & 0 \\ \vdots & \vdots & \vdots & \ddots & \vdots \\ 0 & 0 & 0 & \dots & \omega_n^2 \end{Bmatrix} \tag{22}$$

where $\omega_1=0$, for systems with rigid body modes. Transferring the system from an initial position of $\mathbf{x}_0$ to a final position of rest $\mathbf{x}_r$ results in modal boundary constraints of:

$$\mathbf{y}_0 = \Phi^T \mathbf{x}_0 \tag{23}$$

$$\mathbf{y}_r = \Phi^T \mathbf{x}_r. \tag{24}$$

For controlling the output with high precision, e.g., if the displacement of the final mass of a series of n mass-spring systems is the output, the output equation for the n_{th} mass in modal space is:

$$\mathbf{y}_o = \overbrace{\underbrace{\begin{bmatrix} 0 & 0 & \dots & 1 \end{bmatrix}}_{C_m} \Phi}^{C_o} \mathbf{y} \tag{25}$$

If one is interested in displacement precision, the residual energy of each of the mode is weighted so as to correspond to the same final displacement. For instance, if the contribution to the output displacement of the first two modes are the same, we have the constraint:

$$c_1 y_1 = c_2 y_2 \tag{26}$$

where c_i is the ith component of the modal output matrix C_m. Equation 26 can be transformed to the potential energy space resulting in the equation:

$$c_1^2 \frac{1}{2}\omega_1^2 y_1^2 = c_2^2 \frac{1}{2}\omega_2^2 y_2^2 \left(\frac{\omega_1^2}{\omega_2^2}\right) \tag{27}$$

which states that the potential energy of the second mode has to be scaled by $\frac{\omega_1^2}{\omega_2^2}$ to satisfy the displacement precision constraint. Furthermore, since the output is a linear combination of the modal displacements, the potential energy of each of the modes has to be rescaled by c_i^2 to reflect the modal contribution of every mode.

From the above considerations, we can define indices α_i as:

$$\alpha_i = \frac{c_i^2 \omega_1^2}{5 \; \omega_i^2} \tag{28}$$

to weigh the contribution of each mode in the residual energy equation. The modified cost function for minimax optimization can be written as:

$$V = \sum_{i=1}^{n} \frac{1}{2} \left(\dot{y}_i^2 + \omega_i^2 (y_i - y_i^f)^2 \right) \alpha_i \tag{29}$$

where y_i^f correspond to the desired final state of the ith mode.

4. Robust filter design using weighting factors based on observability measures

Another approach which can be used for determining the scaling factors for the residual energy based cost described in the section 3 is by using modal observability measures proposed by Hamdan and Nayfeh [7]. These observability measures reflect the contribution of respective modes in the desired output and thus can be used for relative scaling of residual energies of each mode. In this scheme the residual modal energy of the system is scaled using observability measures defined as follows:

For the linear system of the form

$$\dot{\mathbf{x}} = A\mathbf{x} + B\mathbf{u}, \mathbf{y}_o = C_o\mathbf{x} \tag{30}$$

A measure of observability of ith mode in the single output defined by C_o is given by

$$\gamma_i = \cos(\phi_i) = \frac{< C_o.p_i >}{\|C_o\|\|p_i\|} \tag{31}$$

where p_i is the ith right eigen vector of A and $< a.b >$ is the inner product of vectors a and b. ϕ_i is the angle between C_o and p_i. This measure gives us the degree to which each mode influences the output. So if the output matrix C_o represents the position of the mass which needs to be precisely controlled then using the above measure, we can calculate the observable measure, which can be used to scale the modal residual energies.

$$w_i = \gamma_i^2 \tag{32}$$

We can then weigh the residual energy of each mode using the above factor and use this as the objective function. For the linear system described by equation 30, the cost function for optimization using the normalized weighing factors can be written as

$$V = \sum_{i=1}^{n} \frac{1}{2} \left(\dot{y}_i^2 + \omega_i^2 (y_i - y_i^f)^2 \right) w_i \tag{33}$$

where y_i is the configuration coordinate for i^{th} mode and y_i^f corresponds to its desired final state.

5. Systems with rigid body modes

For systems with rigid body modes, the technique described in the previous section can be applied after designing a collocated PD feedback control and then shaping the reference input for robust performance. A collocated PD feedback controller is a stabilizing control for the system. Consider the second order system defined in 34 with collocated actuator-sensor pair.

$$M\ddot{\mathbf{x}} + K\mathbf{x} = Du \tag{34}$$

6

where K is positive semi-definite for systems with rigid body modes. Assuming that the null space of the system input matrix D, is not coincident with the null space of K, we can select a candidate Lyapunov function

$$V = \frac{1}{2}(\dot{\mathbf{x}}^T M \dot{\mathbf{x}} + (\mathbf{x} - \mathbf{x}_r)^T K (\mathbf{x} - \mathbf{x}_r) + K_p (\mathbf{x} - \mathbf{x}_r)^T DD^T (\mathbf{x} - \mathbf{x}_r)), \tag{35}$$

where K_p is a positive scalar. The time derivative of V can be written as

$$\begin{aligned} \dot{V} &= \dot{\mathbf{x}}^T (M \ddot{\mathbf{x}} + K (\mathbf{x} - \mathbf{x}_r) + K_p DD^T (\mathbf{x} - \mathbf{x}_r)) \\ &= \dot{\mathbf{x}}^T (D\mathbf{u} + K_p DD^T (\mathbf{x} - \mathbf{x}_r)), \end{aligned} \tag{36}$$

since $K\mathbf{x}_r = 0$. This is due to the fact that the final rest position $\mathbf{x}_r$ lies in the null space of the stiffness matrix K.

If we select the control law as

$$\mathbf{u} = -K_d D^T \dot{\mathbf{x}} - K_p D^T (\mathbf{x} - \mathbf{x}_r) \tag{37}$$

then on substitution of u in 36, $\dot{V}$ reduces to

$$\dot{V} = -K_d \dot{\mathbf{x}} DD^T \dot{\mathbf{x}} \tag{38}$$

which is negative semi-definite since $DD^T \geq 0$. Consequently, the collocated PD controller given by equation 37 is a stabilizing control law for the mechanical system.

6. Results

Two examples are used to illustrate the proposed technique. The first is a three mass-spring system which is similar to the benchmark floating oscillator proposed by Wie and Bernstein [11]. The second examples is based on the double pendulum crane presented by Tanaka & Kuono [10]. For both these examples, a baseline maneuver time was selected to permit an unbiased comparison of the optimal shapers derived by optimizing the modal weighted residual energy cost with the traditional minimax shaped profiles.

6.1. Three mass floating oscillator

Table 1: Reference shaper parameters

Parameter	Method		
	No scaling	Modal disp. scaled	Modal observability scaled
A_0, t_0	0.17,0.00	0.20,0.00	0.18,0.00
A_1, t_1	0.15,1.93	0.12,3.24	0.14,3.01
A_2, t_2	0.27,6.19	0.33,5.87	0.28,5.69
A_3, t_3	0.18,7.97	0.12,8.08	0.16,7.90
A_4, t_4	0.06,10.26	0.04,9.91	0.07,10.07
A_5, t_5	0.16,12.00	0.19,12.00	0.16,12.00

Robust pre-filters for the three mass floating oscillator system with uncertainty in spring constant k as shown in figure 3 were designed using the minimax optimization approach with the scaled residual energy based objective functions for precise rest to rest positioning of mass m_3.
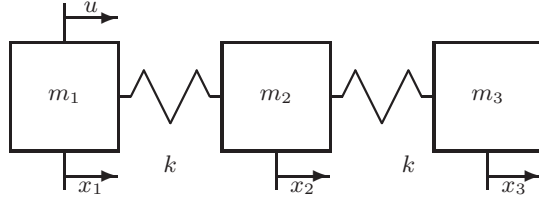
Figure 3: Floating Oscillator

The three mass floating oscillator system shown in figure 3 with $m_1 = m_2 = m_3 = 1$ and $k_{nom} = 1$ is represented by equation 8. To control the position of the three masses, a PD controller with proportional gain of 5 and derivative gain of 0.1 is used. For the purpose of positioning all three masses from an initial position of rest of $(x_1, x_2, x_3) = (0, 0, 0)$, to final position of rest of $(x_1, x_2, x_3) = (1, 1, 1)$ a robust five time delay reference input shaper was used. With modal coordinate transformation, the closed loop system is represented as

$$
\begin{Bmatrix} \ddot{y}_1 \\ \ddot{y}_2 \\ \ddot{y}_3 \end{Bmatrix} + \begin{bmatrix} 0.001 & -0.002 & -0.01 \\ -0.002 & 0.005 & 0.022 \\ -0.01 & 0.022 & 0.094 \end{bmatrix} \begin{Bmatrix} \dot{y}_1 \\ \dot{y}_2 \\ \dot{y}_3 \end{Bmatrix}
$$
$$
+ \begin{bmatrix} 0.33 & 0 & 0 \\ 0 & 2.42 & 0 \\ 0 & 0 & 6.24 \end{bmatrix} \begin{Bmatrix} y_1 \\ y_2 \\ y_3 \end{Bmatrix} = \begin{bmatrix} 0.484 \\ -1.115 \\ -4.85 \end{bmatrix} x_r \tag{39}
$$

where x_r is the position reference to first mass.

Parameters for the reference shaper for a user specified maneuver time of 12 sec, were obtained using minimax optimization based on displacement precision scaled residual energies described in the sections 3 and 4. For comparison purposes the shaper parameters using unscaled residual energy as the objective function were also calculated. These parameters are shown in table 1.

As the output of the system is the position of the third mass, the performance index F, consists of the kinetic energy and pseudo-potential energy of the third mass which goes to zero where $\dot{x}_3$ goes to zero and x_3 equals x_{3r}, the desired final position of mass m_3.

$$
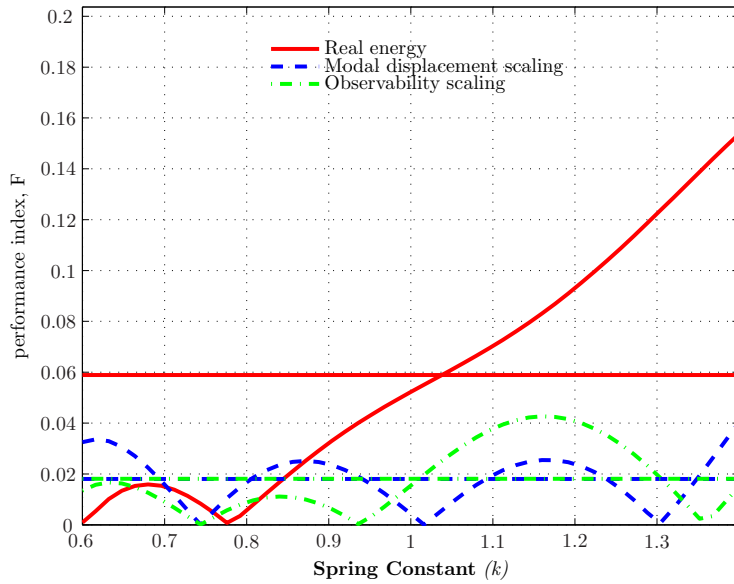F = \frac{1}{2}\sqrt{\dot{x}_3^2 + (x_3 - x_{3r})^2} \tag{40}
$$

Figure 4: Variation of performance index F over the range of parameter variation

Figure 4 illustrates the variation in performance index F evaluated at the end of maneuver, as a function of the uncertain coefficient of stiffness k. for the three types of reference shapers. It is evident from this figure that over the range of parameter variation($0.6 < k < 1.4$), the variation of the performance index F, for the modal displacement based input shaper (dashed line) and observability measure based reference shaper (dash-dot line) is lower than the unscaled residual energy based reference shaper (solid line). Three horizontal lines are also presented which represent the average magnitude of the output energy measure over the uncertain domain for each of the input shaper. This is to permit estimating an average performance over the uncertain domain.
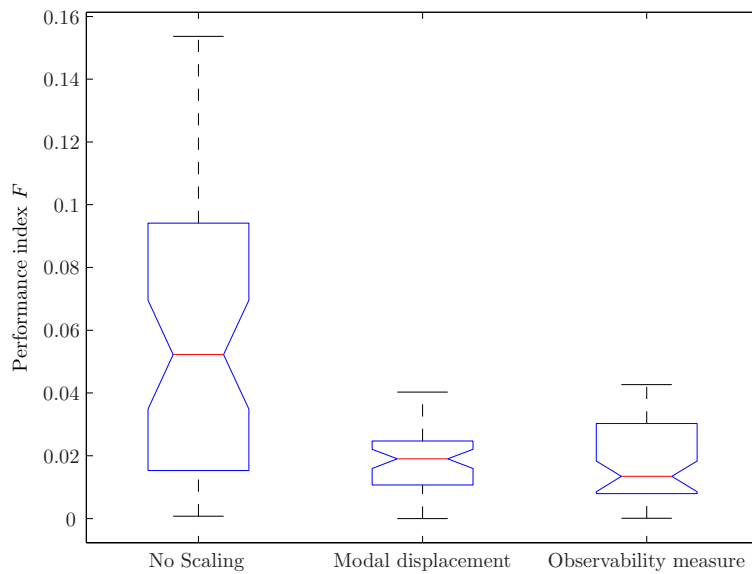
Figure 5: Box plot of performance index F

For better analysis of the performance of the reference shapers over the domain of the uncertain variable,

9

the domain of the uncertainty is sampled uniformly and a box and whisker plot of performance index F for each of the sampled uncertain stiffness k is presented in figure 5. The box and whisker plots are traditionally used to display statistical properties of data using a five number summary (upper and lower quartile, sample minimum and maximum, and median). The upper and lower lines of the box represents the upper and lower quartile respectively. The line at the notch represents the median value and the whiskers extending from the edge of the box represent the extreme values. It is clear from this plot that modal displacement and observability scaled controllers perform much better than the original residual energy based controller. In conclusion, of the three controllers the maximum magnitude and variation of the performance index F, is the lowest for modal displacement based controller

Figure 6 shows the shaped reference input profile for the three methods which illustrate significantly different switch times which is reflected in different location of the zeros of the time-delay filter.
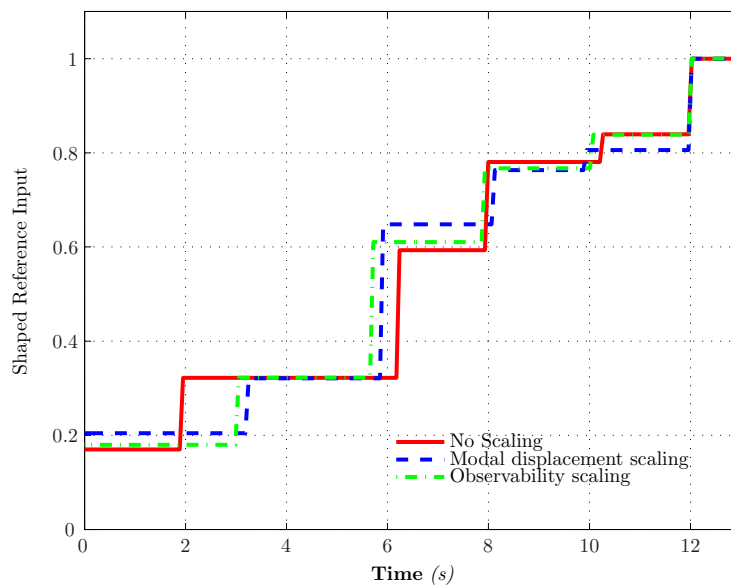

Figure 6: Shaped reference input profile for 3 mass floating oscillator

The response of the third mass at nominal value of spring constant $k=1$ using the three shaped inputs is shown in figure 7. As is apparent from the figure, the position of third mass is more precisely controlled by the scaled energy filters as compared to the traditional minimax filter which does not scale the residual energy.
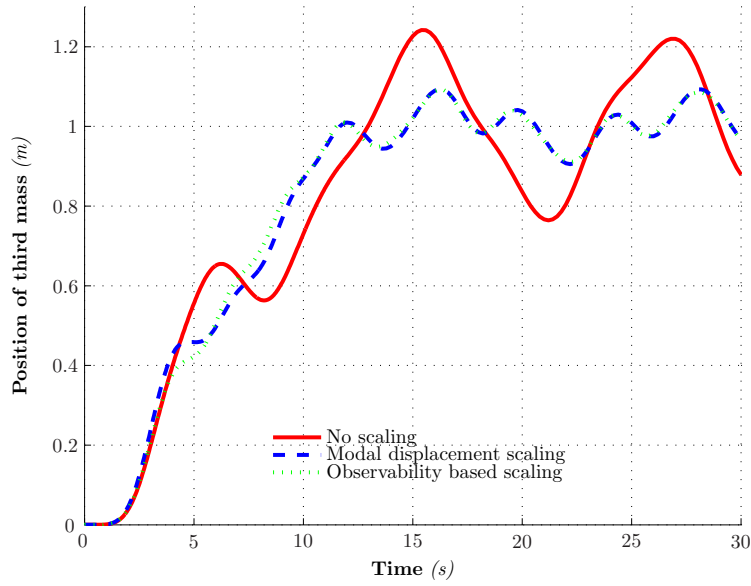
Figure 7: Response of second mass to different types of filters at nominal k

The box plots for scaling factors evaluated using the two approaches are shown in figure 8. The plots illustrate the variation in these scaling factors with change in the uncertain parameter k. Both modal displacement and observability measures based factors assign large weights to the first mode (lowest frequency) and small weights to the third mode (highest frequency). Further, the variation of these factors with change in uncertain parameter is higher for the observability measure based scaling illustrated by the size of the box and whisker plots.
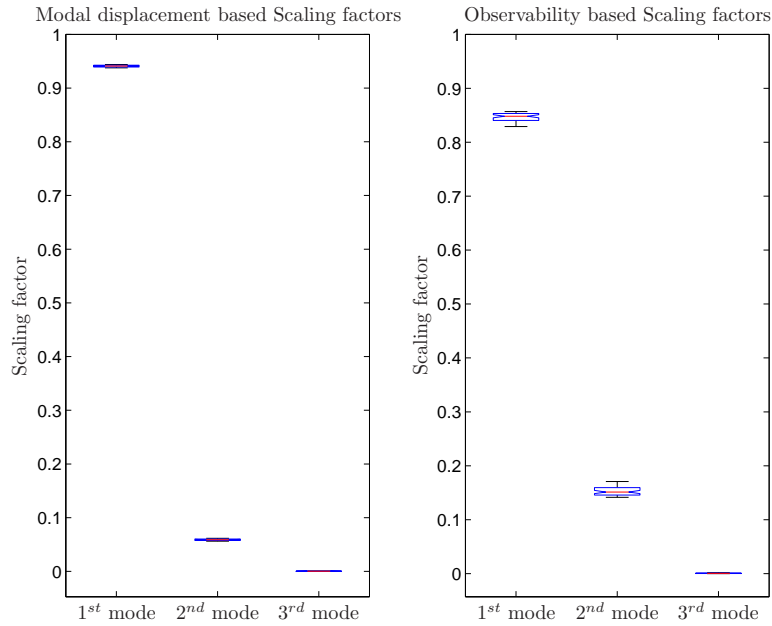

Figure 8: Box plot showing the variation of scaling factors over the range of parameter variation

Effect of these scaling factors can also be seen in the placement of controller zeros in figure 9. Controller

zeros for the scaled residual energy methods ($\diamond$ and $\triangle$) are placed to cover the spread of system poles corresponding to the first and second modes and ignores the third mode whereas the original residual energy based controller ($\circ$) distributes the zeros around all three modes. The series of dots in Figure 9 illustrate the root locus of the system poles as a function of the uncertain stiffness coefficient k.
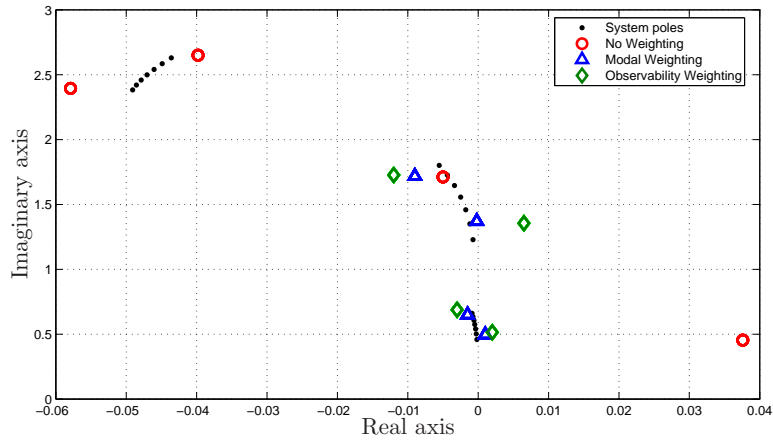

Figure 9: Zeros of Time-delay Filters

6.2. Gantry crane

As a second example case, a double-rigid-body pendulum gantry crane model proposed by Tanaka & Kuono [10] shown in figure 10 is considered.
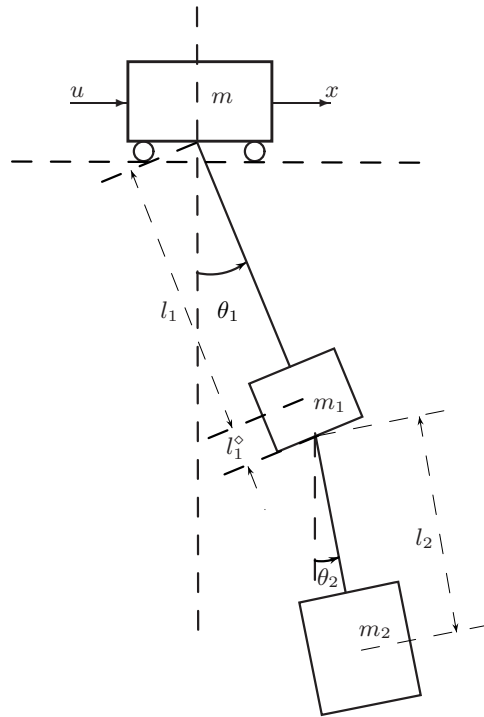

Figure 10: Double-rigid-body pendulum gantry crane model

12

Parameter	Value
m	$8kg$
m_1	$0.5kg$
m_2	$6kg$
l_1	$1.5m$
$l_1^\diamond$	$0.1m$
l_2	$0.3m$
I_1	$.0008kg\ m^2$
I_2	$0.06kg\ m^2$
a	$1.0Nm/s$

The equations of motion for the system assuming θ_i and $\dot{\theta}_i (i = 1, 2)$ to be small can be written as

$$c_{11}\ddot{x} + c_{12}\ddot{\theta}_1 + c_{13}\ddot{\theta}_2 + a\dot{x} = u \tag{41}$$

$$c_{21}\ddot{x} + c_{22}\ddot{\theta}_1 + c_{23}\ddot{\theta}_2 + c_{24}\theta_1 = 0 \tag{42}$$

$$c_{31}\ddot{x} + c_{32}\ddot{\theta}_1 + c_{33}\ddot{\theta}_2 + c_{34}\theta_2 = 0 \tag{43}$$

where

$c_{11} = m + m_1 + m_2$, $c_{12} = m_1 l_1 + m_2(l_1 + l_1^\diamond)$

$c_{13} = m_2 l_2$, $c_{21} = m_1 l_1 + m_2(l_1 + l_1^\diamond)$

$c_{22} = m_1 l_1^2 + m_2(l_1 + l_1^\diamond)^2 + I_1$, $c_{23} = m_2 l_2(l_1 + l_1^\diamond)$

$c_{24} = m_1 g l_1 + m_2 g(l_1 + l_1^\diamond)$, $c_{31} = m_2 l_2$

$c_{32} = m_2 l_2(l_1 + l_1^\diamond)$, $c_{33} = m_2 l_2^2 + I_2$, $c_{34} = m_2 g l_2$

Table 2 lists the crane model parameters. To control the position of the trolley, a PD controller with proportional gain of 10 and derivative gain of 1 was used. Robust pre-filters for shaping the position reference when there is uncertainty in the length ratio l_1/l_2, were designed using the aforementioned methodologies. The system needs to be positioned from initial value of $(x_1, \theta_1, \theta_2) = (0, 0, 0)$ to $(x_1, \theta_1, \theta_2) = (1, 0, 0)$. In this scenario, we are interested in reducing the sway of the payload at the end of the trolley-positioning maneuver, y_o. So the emphasis is on the precise control of the payload displacement given by equation.

$$y_0 = (l_1 + l_1^\diamond)\theta_1 + l_2\theta_2 \tag{44}$$

Parameters for the reference shapers designed using the three methodologies for a fixed final time of 6 seconds are shown in table 3

The output of the system here is the position of the payload. So the performance measure, F, used here

Table 3: Reference shaper parameters

Parameter	Method		
	No scaling	Modal disp. scaled	observability scaled
A_0, t_0	0.098,0.000	0.102,0.000	0.101,0.000
A_1, t_1	0.248,0.795	0.253,0.815	0.254,0.847
A_2, t_2	0.214,1.692	0.202,1.669	0.203,1.707
A_3, t_3	0.184,4.275	0.179,4.265	0.174,4.292
A_4, t_4	0.194,5.183	0.197,5.137	0.196,5.153
A_5, t_5	0.064,6.000	0.067,6.000	0.071,6.000

is the total energy of the payload.

$$F = KE + PE \tag{45}$$

$$PE = m_2 g[(l_1 + l_1^\diamond)(1 - cos\theta_1) + l_2(1 - cos\theta_2)] \tag{46}$$

$$KE = \frac{1}{2}[m_2(\dot{x}_{cm2}^2 + \dot{y}_{cm2}^2) + I_2\dot{\theta_2}^2] \tag{47}$$

$$x_{cm2} = (l_1 + l_1^\diamond)sin\theta_1 + l_2 sin\theta_2 \tag{48}$$

$$y_{cm2} = -(l_1 + l_1^\diamond)cos\theta_1 - l_2 cos\theta_2 \tag{49}$$
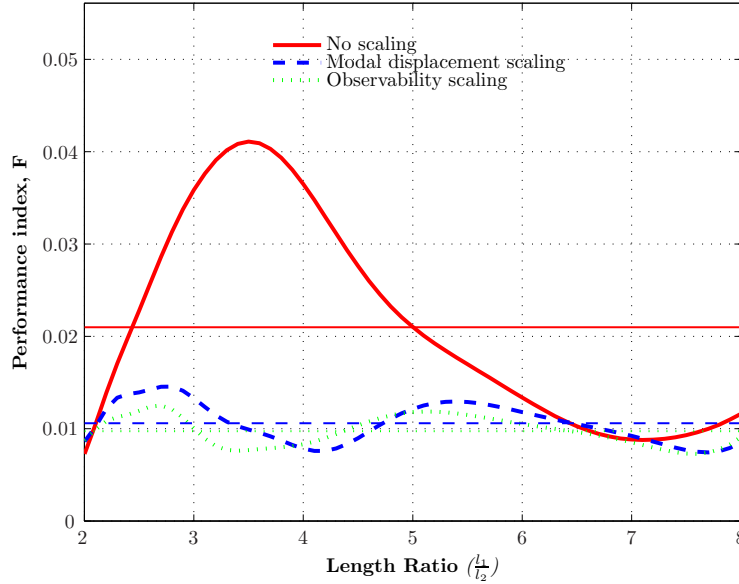

Figure 11: Residual output vibration distribution for Gantry crane model with variation in length ratio (Nominal $l_1/l_2 = 5$)

Figure 11 shows the sensitivity measure for the displacement of the payload $(l_1 + l_1^\diamond)\theta_1 + l_2\theta_2$ to variation in the length ratio l_1/l_2, for the three types of reference shapers. We again see that over the range of parameter variation $(2 < l_1/l_2 < 8)$ profiles obtained using the modal displacement based scaling (dashed line) and observability measures based scaling (dotted line) for the cost function show improvement over the real energy based cost function (solid line). The horizontal line are illustrated to represent the average performance of each of the input shaper over the uncertain domain.
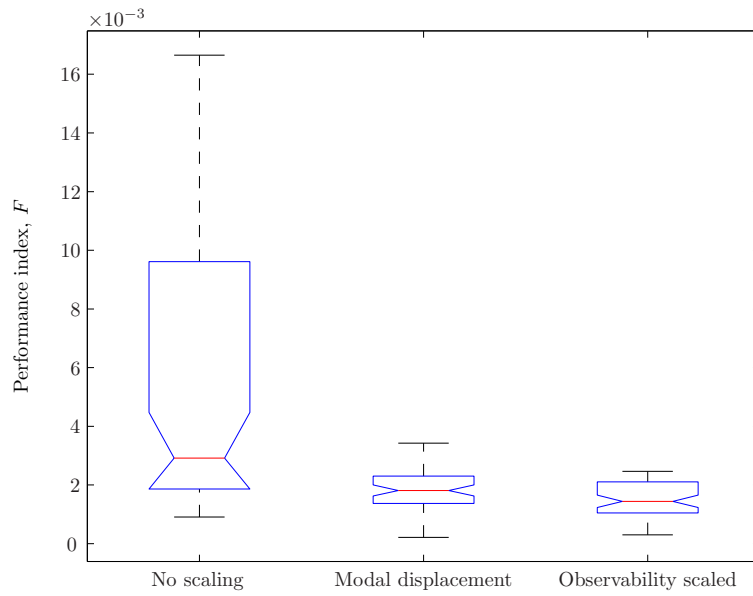
Figure 12: Box plot of performance index F at the end of maneuver for Gantry crane system

A box and whisker plot of the performance index F evaluated for uniformly sampled variation of the length ratio l_1/l_2, at the final time is presented in figure 12. We again see that the performance of modal displacement based and observability measures based controllers is much better than the original residual energy based controller. Out of the three controllers the maximum magnitude and variation of the performance index F, is lowest for observability measure based controller.

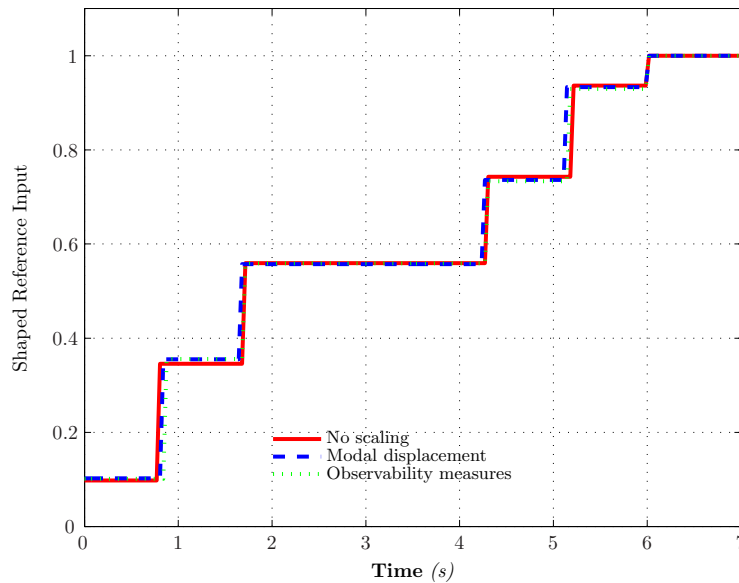Figure 13 shows the shaped reference input profile obtained using the three methods.

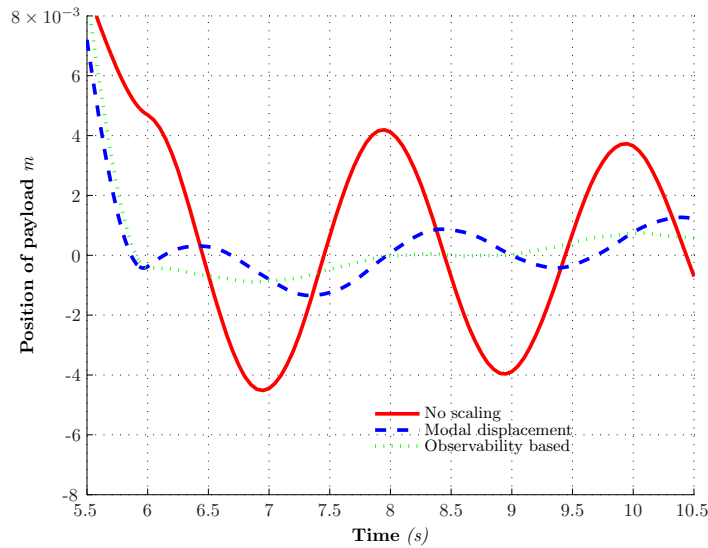Figure 13: Shaped reference input profile for Gantry crane model

15

Figure 14: Response of payload to different types of filters at nominal length ratio($l_1/l_2 = 5$)

The displacement of the payload for nominal value of length ratio ($l_1/l_2 = 5$) using the three kinds of input is shown in figure 14 in the proximity of the end of the maneuver (6 sec). As is apparent from the figure, the response corresponding to modal displacement and observability measure based reference filters is better than the unscaled residual energy based filter.
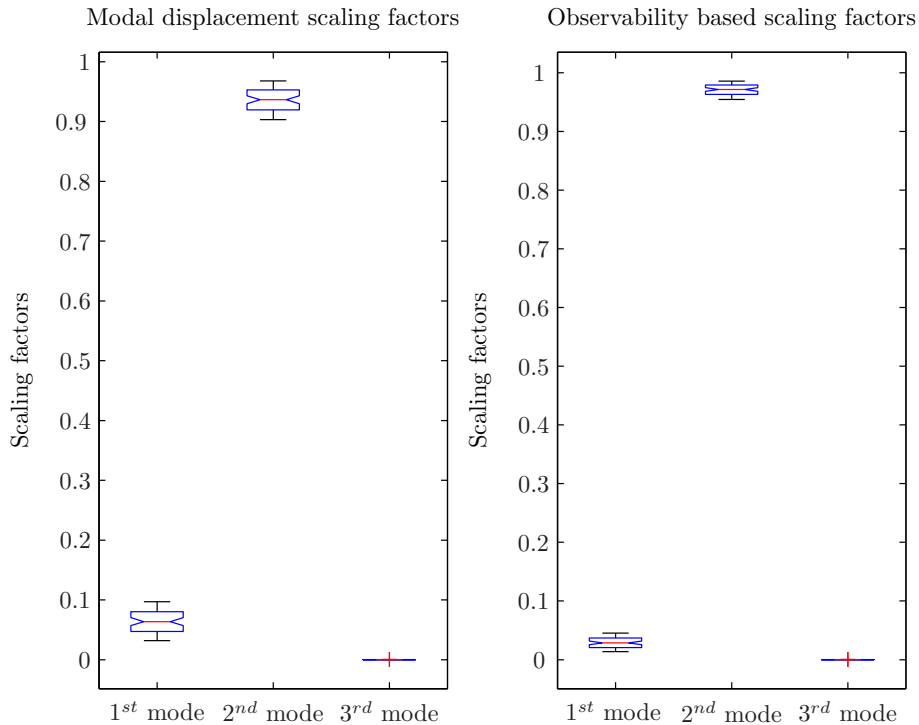

Figure 15: Box plot showing the variation of scaling factors over the range of parameter variation

A box and whisker plot showing the scaling factors corresponding to variation in length ratios, l_1/l_2, uniformly sampled from the uncertain domain is illustrated in Figure 15. Both scaled energy methods assign larger weights to the second mode and very small weights to the third mode. Also, the variation in the

16

weights is larger for modal displacement based scaling compared to observability measure based scaling.

7. Conclusions

In this paper we proposed two methods of scaling the cost used in the minimax optimization based design of robust input shapers for multi-mode systems. The weighing factors were derived based on the relative importance of respective modes in the output. The proposed techniques were then demonstrated on a three mass floating oscillator and a double pendulum gantry crane model. It was shown that for these examples, the residual vibration sensitivity measures are lower for reference shapers designed using scaled costs as compared to the shapers designed using the real residual energy as the cost for optimization.

References

[1] Sorensen, K. L. and Singhose, W. E., "Command-induced vibration analysis using input shaping principles", *Automatica*, Vol. 44, No. 9, 2008, pp 2392-2397.

[2] Singhose, W., Kim D., and Kenison, M., "Input shaping control of double-pendulum bride crane oscillations", *ASME Journal of Dynamic Systems, Measurement and Control*, Vol. 130, 034504, 2008.

[3] Smith, O. J. M., "Posicast Control of Damped Oscillatory Systems", *Proc. of the IRE*, 1957, pp 1249-1255.

[4] Singer, N. C., and Seering, W. P., "Preshaping Command Inputs to Reduce System Vibrations", *ASME Journal of Dynamic Systems, Measurement and Control*, Vol. 112, 1990, pp 76-82.

[5] Singh, T., Vadali, S. R., "Robust Time-Delay Control of Multimode Systems", International Journal of Control, Vol. 62, No. 6, 1995, pp 1319-1339.

[6] Singh, T., *Minimax Design of Robust Controllers for Flexible Systems*, Journal of Guidance, Control and Dynamics, vol. 25, No. 5, pp. 868-875, 2002.

[7] Hamdan, A. M. A. and Nayfeh, A. H., "Measures of modal controllability and observability for first- and second-order linear systems," Journal of Guidance, Control, and Dynamics, vol. 12, no. 3, pp. 421-428, 1989.

[8] Kenison, M., and Singhose, W., "Input Shaper Design for Double-Pendulum Planar Gantry Cranes", Proceedings of the 1999 International Conference on Control Applications, Hawaii, Hawaii.

[9] Manning, R., and Singhose, W., "Frequency Variations and Control of Two-Link Robot Arms with Varying Payloads", Proceedings of the 2008 International Symposium on Flexible Automation, Atlanta, GA.

[10] Tanaka, S. and Kouno, S., "Automatic measurement and control of the attitude of crane lifters", Control Engineering Practice 6, pp. 10991107, 1998

[11] Wie, B. and Bernstein, D., "Benchmark Problems for Robust Control Design", *J. of Guidance, Control and Dynamics*, Vol. 15, No. 5, 1992, pp 1057-1058.

[12] Pao, L. Y., Chang, T. N., and Hou, E., "Input Shaper Design for Minimizing the Expected Level of Residual Vibration in Flexible Structures," Proceedings of the 1997 American Control Conference, American Automatic Control Council, Evanston, IL, 1997, pp 3542-3546.